JOURNAL OF AIRCRAFT
Vol. 42, No. 4, July–August 2005

Thrust-Matching Requirements for the Conceptual Design of Hypersonic Waverider Vehicles

Kashif H. Javaid* and Varnavas C. Serghides†
Imperial College London, South-Kensington Campus, London, England SW7 2AZ, United Kingdom

A methodology is presented that integrates a turboramjet and scramjet with a conically derived waverider airframe to achieve sustained hypersonic flight. A smooth transition between the two powerplants is achieved by calculating the performance and matching the thrust during the appropriate Mach regime. The engines are modeled using a one-dimensional approach, and a streamline tracing technique is employed to generate the lower surface of the waverider. Propulsion/airframe integration issues are discussed with a two-dimensional analysis of the inlet and nozzle. Results are presented for a turboramjet operating from static to Mach 5, for a turboramjet/scramjet combination at transition speeds and for a scramjet alone during constant altitude acceleration to Mach 10 at 30 km. A Mach 10 example waverider, maximized for the lift-to-drag ratio, produced a value of 7.8. This was selected to illustrate that performance can be rapidly predicted using this design methodology.

Nomenclature

A	=	capture area
A/A^*	=	isentropic area ratio
ae	=	semiminor axis of inlet curve
be	=	semimajor axis of inlet curve
D	=	drag
F/m_0	=	specific thrust
H	=	height
h	=	altitude
I_{sp}	=	specific impulse
L	=	lift
L_{fore}	=	length of forebody
M	=	Mach number
$\dot{m}$	=	mass flow rate
P	=	pressure
R	=	radius
T	=	temperature
V	=	velocity
$v(M)$	=	Prandtl–Meyer function
W	=	width
α	=	turboramjet bypass ratio
γ_b	=	specific heat ratio
δ	=	streamline deflection angle
ϵ	=	bow shock angle
η_R	=	inlet total pressure recovery
θ	=	semispan angle
π_F	=	turboramjet total pressure ratio
0	=	freestream
1	=	inlet capture
2–10	=	engine station numbers

Subscripts

d	=	downstream
eng	=	engine at inlet plane
i	=	inlet station
p	=	turboramjet primary flow
r	=	radial
req	=	required engine airflow
shock	=	shock position at given station
t	=	total
u	=	upstream
wing	=	wing curve
x	=	axial station

Presented as Paper 2003-6953 at the AIAA 12th International Space Planes and Hypersonic Systems and Technologies, Norfolk, VA, 15–19 December 2003; received 4 March 2004; revision received 2 July 2004; accepted for publication 7 June 2004.

*Research Student, Department of Aeronautics, South-Kensington Campus. Student Member AIAA.

†Lecturer, Department of Aeronautics, South-Kensington Campus. Senior Member AIAA.

Introduction

THE potential benefits of an airbreathing hypersonic vehicle are apparent for both the commercial and military domain. Routine, affordable, and flexible access to space remains a high priority in order to reduce the invariably high cost of sending a payload into low-Earth orbit. Through the use of airbreathing engines, the overall efficiency of reusable launch vehicles is increased as a result of the reduced volume of required onboard propellant. For future military aerospace systems, there are obvious advantages of delivering a payload at hypersonic speeds and with global range. The missions extend from tactical to strategic and have applications from access to space, reconnaissance/surveillance to rapid global response.[1]

The interest in airbreathing propulsion systems for future hypersonic aerospace vehicles arises from their potential to extend the operational envelope for improved overall system performance efficiency. Such powerplants will use atmospheric oxygen for propulsion over the largest part of an endoatmospheric mission trajectory, and extensive research has been conducted on integrating such systems on hypersonic vehicle configurations.

NASA's X-43A hypersonic research aircraft flew at the world-record speed of Mach 7 in March 2004, which is an example of a Scramjet (SJ) integrated with a lifting-body airframe.[2] As demonstrated by the test, the propulsion system has a large impact on the configuration design of a hypersonic cruise vehicle. The entire undersurface of the vehicle behaves as the propulsion system with the forebody providing the compression for the combustor and the aftbody acting as the thrust surface. Such a vehicle will travel at high altitudes, where the air density is low and the freestream capture area required for effective combustion is large.

The objective of the current research program is to develop a conceptual methodology that facilitates the rapid design and analysis of an uninhabited hypersonic vehicle. It should be capable of horizontal takeoff and landing with rapid turnaround times. The need for an uninhabited operational vehicle intended for such applications arises through consideration of the benefits resulting from the elimination of constraints associated with crew/passenger accommodation.

To maximize range for cruise-type applications as considered in this study, the lift-to-drag (L/D) ratio is a good aerodynamic figure of merit. One class of vehicles that deliver high L/D ratios is waveriders; first presented by Nonweiler[3] and later proved their capacity for low-drag characteristics using viscous analysis.[4] They are generated using an inverse generation process from a prescribed supersonic flowfield.

At some specified design Mach number and altitude, the bow shock wave that is produced is attached all along its leading edge, and that isolates the top surface from the lower compression surface. The properties of the inviscid flowfield at the inlet face are then known precisely, which enables the waverider to be designed for governing flow variables. This shock attachment reduces flow spillage and pressure loss, thereby increasing efficiency. An added advantage is that they can be generated with minimum computational expense.

Existing engine-airframe integration studies[5] have shown how a SJ is integrated with a conically derived waverider[6] and an osculating-cone waverider[7] geometries. These waveriders have been optimized for L/D and produced favorable results over comparable lifting-body concepts. Waveriders perform well during off-design conditions,[7] and practical issues such as leading-edge blunting can be accommodated with only a small drop in L/D.

The design challenge posed by this type of vehicle is considerable because of the wide operating conditions it will experience. Tight integration of multiple aircraft systems is required to meet the high-performance requirements and overall success of a concept. The complete undersurface of the vehicle contributes to the propulsion system of the vehicle to generate sufficient thrust. The thrust requirements are related to engine size, which in turn is dependent on the vehicle airframe size and design. Therefore, the success of a hypersonic vehicle is critically dependent on how well the propulsion system is integrated with its airframe.

The waverider forebody thus behaves as the inlet/compression system to provide the inlet area and necessary mass flow for SJ combustor requirements. The other major feature of the integrated configuration and external to the engine is the aftbody and is used as an extension to the nozzle. This allows higher engine exhaust velocities with modest area expansion in the nozzle area, thereby producing low drag.

The forebody/inlet compression effectively reduces the required engine size and weight requirements compared to a freestream inlet; the inlet compression increases the overall engine efficiency. As the engine forces are distributed along the vehicle undersurface, the airframe lift, drag, trim, and control requirements will depend directly on the engine characteristics. The undersurface not only generates thrust, but pitching moment and lift, particularly the nozzle providing minimal aerodynamic drag. The main body of the waverider structure will contain the propellant.

Two types of engines will be required to achieve hypersonic speed: one for the low-to-high supersonic flight and one for the hypersonic regime. Current airbreathing engines are prevented from operating at hypersonic speeds because of high heating loads and dissociation losses. A SJ is designed to maintain supersonic flow inside the engine, but the difficulty arises during combustion where the residence times are short.

The hypersonic propulsion system is a hydrogen-burning SJ engine, which is required for the high-speed segment of the mission M_0 between 5 and 9/10. Turboramjets (TRJs) are used to accelerate the vehicle from brakes release through subsonic, transonic, and up to high supersonic flight Mach numbers until safe transition to the hypersonic SJ mode is established. Mach 5 is considered to be the limit of the TRJ's efficient operation because of high-temperature effects and inefficient compression. The TRJ is an example of a turbine-based combined-cycle (TBCC) type engine and was selected its near-term potential[8,9] and to avoid installing separate turbojet and ramjet systems. This saves on dead weight considering the turbojet becomes inefficient above Mach 3. Furthermore, a TRJ will be more fuel and volume efficient and will also help to avoid the extra complexity associated with the added transition from turbojet to ramjet. In this paper, the term low-speed powerplant will represent the TRJ operating between $0 \leq M_0 \leq 5$ and high speed will demonstrate the SJ at speeds of $5 < M_0 \leq 10$.

This paper seeks to investigate the integration of multiple airbreathing engines and flowpaths as just described onto a waverider airframe to account for the full flight path from takeoff to hypersonic cruise. To ensure quick computation time, the SJ and TRJ are modeled using quasi-one-dimensional flow, and the nozzle is modeled with frozen exhaust flow. The relationship of lift and drag on the waverider design is analyzed, and details of the methodology employed are presented for achieving a smooth thrust transition from the low-speed to high-speed engine. There is a tradeoff between producing thrust and maximizing L/D, which is the function of the optimization. Analysis is carried out on generating maximum L/D waverider shapes with a Mach 10 example.

The ultimate goal of this study is to present a design methodology that accounts for fully integrated aircraft subsystems enabling an optimized design to given initial inputs. This method of design and optimization allows for rapid prediction of performance, aerodynamics, and, most importantly, reduced design cycle times.

Automated Design Procedure

During the conceptual design stage of a hypersonic vehicle, many parameters need to be analyzed concurrently, and the vehicle needs to be fully integrated in design, functions, and operation. Owing to the strong coupling of the external vehicle aerodynamics/propulsion and performance of the vehicle, a multidisciplinary solution is only viable if a rapid exploration of the design space is achievable. The approach adopted for this study focuses on the use of simple models, first principles, and estimates in order to overcome certain uncertainties associated with current limitations of the aerospace design methodologies. Computationally based interactive design algorithms relevant to hypersonic design that address three-dimensional viscous flow phenomena are very costly because of the large computational resource required.

From the preceding argument, the design space is large owing to the interdependence of aircraft subsystems, thereby requiring multidisciplinary optimization to produce optimum designs.[10] Some early complete design methodologies considered simple geometric shapes that did not account for the three-dimensional nature of the hypersonic flowfield[11–13] or focused only on the on-design case.[14] Newer methods have looked at detailed engine-airframe integration and optimization, as discussed earlier, for the high-speed segment and the rocket-based combined-cycle engine (RBCC) for the full Mach range.[15]

To address the need of a method from a designers perspective, Hypersonic Interactive Combat Aircraft Design (HICAD) is being developed as part of a Ph.D. program at Imperial College London. HICAD is an interactive visual environment application, written in MFC[16] and C++, that allows the user to explore the impact of initial design parameters such as the Mach number, cruise altitude, and waverider forebody shock angle. There is capacity for multivariable optimization, a necessary component of the design cycle to account for the nonlinearity. Therefore, a wide range of vehicle concepts can be rapidly explored in HICAD by reducing the initial design cycle time as compared to detailed and expensive computational-fluid-dynamics (CFD) component analysis.

An example mission profile relevant to the current study is illustrated in Fig. 1. The vehicle will be designed to takeoff, accelerate, and climb using an array of TRJs until the desired cruise altitude specified by the user is achieved at Mach 5. Prior to this, the TRJ propulsion system will continue operating in parallel with the SJ, and when thrust matching is achieved (near Mach 5) the airflow to the TRJ is shut off. The SJ then throttles up, and the aircraft begins a constant-altitude acceleration to the desired cruise Mach number. At the end of the cruise segment, the vehicle will slow down and revert to TRJ power, descend to a specified altitude, deliver its payload, and fly to a base for refueling.

The computational steps taken in designing a complete and operational vehicle are shown in Fig. 2. The design begins by performing an initial sizing routine that is dependent on the user-selected basic requirements as explained earlier. Elements such as the mission

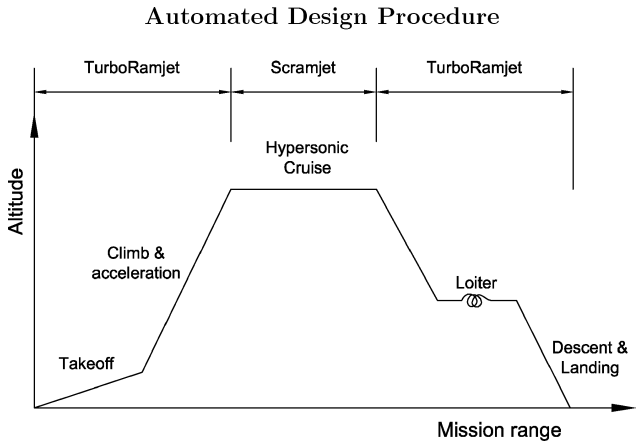

Fig. 1 Basic mission profile for a hypersonic cruise vehicle.

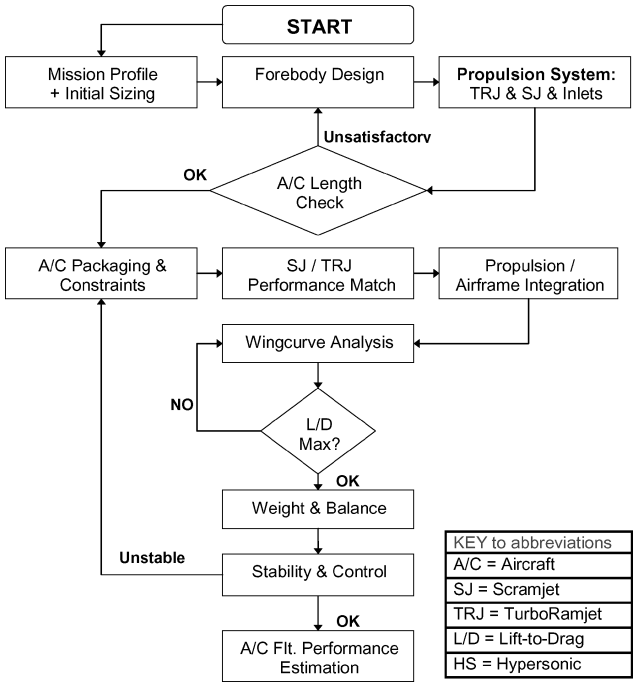

Fig. 2 Flowchart illustrating the processes with the automated initial design methodology.

profile and aircraft constraints are laid out. L_{fore} is then determined using the streamline tracing method, which also requires certain user inputs that will be described later. Given an acceptable L_{fore}, the SJ inlet size is determined for the on-design case from a predefined combustor pressure ratio. This undergoes an iteration process with optimized values being computed for inlet ramp angle, inlet height, flow properties at the inlet/combustor junction, and the capture area. The SJ computation then proceeds with the ideal combustor analysis and concludes with the determination of the nozzle flowfield.

For the low-speed segment of the mission, the TRJ analysis begins by determining the specific thrust at different altitudes using an idealized analysis. The size of the low-speed inlet is then calculated from the design M_0 and $\dot{m}_0$ variation with h, using an external code that is integrated with HICAD. The required area ratio with respect to the design A_0 is plotted for different altitudes, and the most demanding $\dot{m}_0$ and h values are used to size the inlet. For the majority of cases studied, that point was at Mach 5/cruise altitude transition to SJ mode. Once the inlet size and ramp angles are determined for the off-design conditions, fuel and other systems are accommodated into the vehicle's volume.

The TRJ and SJ analyses are iterative. The design $\dot{m}_0$ for the TRJ and the W_{eng} for SJ (amongst other parameters, discussed in the ensuing sections) are adjusted until I_{sp} and thrust matching is achieved with a smooth transition between the two powerplant modes. Following the completion of an optimization loop for thrust matching, the remaining vehicle is designed, which includes the wing section from nose to tail. The same streamline tracing technique is used after specifying a wing curve at the tail plane. The curve shape is varied until a maximum L/D configuration is achieved, which is aided by a force accounting procedure. The inlets of the TRJ and SJ are then positioned in a over/under arrangement[9,17,18] so that the powerplants can operate independently of each other. Once the vehicle and its systems have been packaged together, its stability, mission, and field performance can be calculated, including off-design conditions.

Waverider Forebody

The conical shock produced from a right circular cone at the desired M_0 prescribes the flowfield for the inverse design of a waverider. A forebody designed this way minimizes pressure leakage from the lower surface and maximizes the mass flow captured by the engine for a given altitude. A planar ramp is integrated into the forebody such that the planar shock it generates impinges on the cowl in order to increase flow uniformity for the combustor. The closer the cowl is to the shock, the greater the mass capture.

The forebody shape and length L_{fore} are determined from an inlet curve corresponding to a segment of an ellipse with a lateral spacial limit equal to W_{eng} as shown in Fig. 3. A greater ellipticity of the inlet curve results in an increase forebody length.

By specifying ϵ and R_{shock} in the inlet plane, the axial location of the inlet plane and cowl lip is determined. The cowl lip is positioned such that it is in contact with R_{shock} at the inlet plane.

In contrast to the conical flowfield, which is readily computed and appropriate for producing rapid configurations, an osculating cone flowfield, originally developed by Sobieczky et al.,[19] can be prescribed and used to generate a different class of waverider. The nonaxisymmetric shock definition is conical in the osculating plane, and a series of planes along the shock curve are used to fully define the flowfield. This is a more complex method of computing a flowfield thereby increasing the computational cost especially when searching for optimized configurations requiring many iterations. There are, however, limitations to the conically derived flowfield in that the usable volume is significantly greater, but the L/D ratio is comparable.[20]

The conical flowfield is determined by solving the Taylor–Maccoll ordinary differential Eq. (1) for supersonic flow using a fourth-order numerical Runge–Kutta technique[21]:

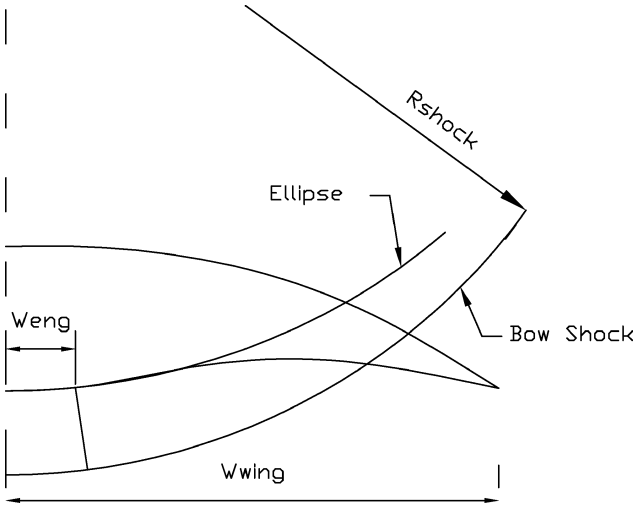

Fig. 3 Waverider initial design parameters at the inlet plane.

$$\frac{\gamma-1}{2}\left[1-V_r'^2-\left(\frac{\mathrm{d}V_r'}{\mathrm{d}\theta}\right)^2\right]\left[2V_r'+\frac{\mathrm{d}V_r'}{\mathrm{d}\theta}\cot\theta+\frac{\mathrm{d}^2V_r'}{\mathrm{d}\theta^2}\right]$$
$$-\frac{\mathrm{d}V_r'}{\mathrm{d}\theta}\left[V_r'\frac{\mathrm{d}V_r'}{\mathrm{d}\theta}+\frac{\mathrm{d}V_r'}{\mathrm{d}\theta}\frac{\mathrm{d}^2V_r'}{\mathrm{d}\theta^2}\right]=0 \quad (1)$$

where V_r and θ are the two independent variables and $V_\theta = \mathrm{d}Vr'/\mathrm{d}\theta$. Streamlines are traced forward from the inlet curve until the bow shock is intersected, and this is repeated spanwise for W_{eng}. These streamlines form the lower surface of the waverider for the span of the engine—an input by the user and an adjustment for smooth thrust transition (see Results section).

Outboard Waverider Definition

This area is known as the wing curve and represents the design space from W_{eng} to the shock radius at the tail plane. The wing curve is generated by fitting a third-order polynomial through several points defined at the tail station as explained by O'Neill,[6] three of which are the outboard-most points traced from the elliptical section at the inlet plane to tail plane. The wing curve at the tail plane then forms the initial points to trace forward in a similar fashion to the forebody part until the bow shock is intersected. Certain constraints on the tail station points are necessary such that the design space does not extend beyond R_{shock} nor lie within the generating cone. In addition, the wing curve points should not produce a concave leading edge when traced forward of the tail plane, and the point on the shock at the tail plane is constrained to be less than the cowl radius to avoid an excessive landing gear height.

The resulting three-dimensional shape is illustrated in the schematic of Fig. 4, and it appears that the vehicle is riding its shock wave attached to the waverider leading edge.

L_{fore} variation with Mach number is shown in Fig. 5 for varying ϵ. In general, the length appears to increase linearly with M_0 for given values of ae, be, and R_{shock}.

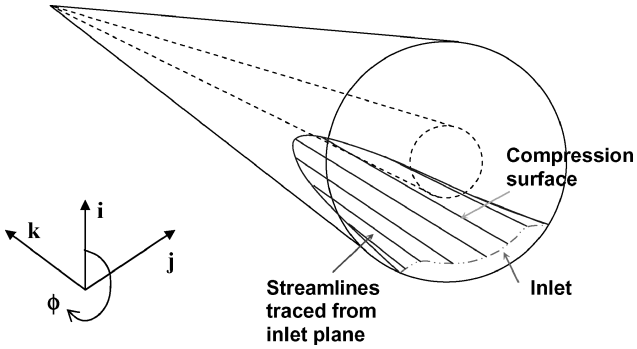

Fig. 4 Forebody generation using an inverse design approach starting at the inlet plane; adapted from Ref. 1.

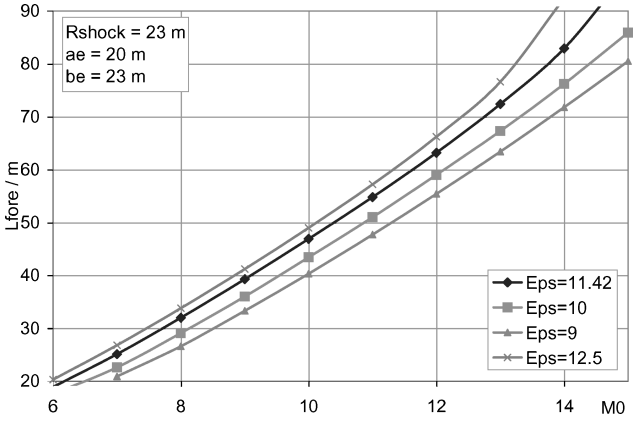

Fig. 5 Forebody length variation for multiple shock angles.

Table 1 Inlet/combustor junction flow properties

M_0	P, Pa	T, K	M_i	H_i
6	41,460	715	2.73	0.496
7	55,737	773	3.20	0.457
8	71,228	833	3.62	0.454
9	87,098	893	4.01	0.456
10	106,504	970	4.33	0.436
11	125,916	1,047	4.63	0.435
12	148,538	1,137	4.88	0.438
13	169,428	1,224	5.13	0.431
14	196,385	1,333	5.31	0.427

For this study, the upper surface is simply aligned with the freestream direction by tracing back from the leading-edge curve to the base of the vehicle. The pressure is therefore equal to the freestream pressure p_∞.

The intake is one of the most critical components of an airbreathing engine, and it should be properly shaped to accommodate the unstable nature of supersonic combustion. In addition to the compression provided by the bow shock of the waverider forebody, inlet ramps and the reflected shock off the cowl lip are used to further compress the flow according to the inlet requirements. Inlet shock instabilities caused by high backpressures from combustion are a current area of research. A thorough account of the inlet flow requires detailed CFD analysis, which is beyond the scope of this study.

The axisymmetric flowfield produced by the conical shock is transformed into two-dimensional flow by using a single planar inlet ramp as explained earlier. This maintains flow uniformity inside the combustor, minimizing the three-dimensional effects especially at the inlet/combustor interface. The forebody thermodynamic variables are mass averaged to enable a two-dimensional oblique shock calculation to be carried out to maintain a shock-on-lip condition at the engine design Mach number (see Fig. 6). The ramp angle is varied iteratively, and the mass-averaged values are used to determine the strength of the ramp shock and reflected cowl shock until the desired inlet pressure ratio is achieved as given by Eq. (2) in Ref. 22.

$$P_i/P_0 = -8.4 + 3.5M_0 + 0.63M_0^2 \quad (2)$$

The reflected shock cancels on the upper wall of the combustor while turning the flow parallel to the cowl. Its angle is kept the same as the angle the streamline makes with the freestream flow once it passes through the bow shock. Table 1 shows the on-design flow properties after the inlet shock system. A movable cowl can be used to maintain a shock-on-lip condition for off-design considerations, but that is not considered in this paper.

Scramjet Combustor

Research efforts[9,18,22] and the recent NASA success[3] suggest that a hydrogen-fueled SJ offers the greatest near-term development potential for the high-speed segment of the mission. The SJ is modeled based on the following assumptions: 1) quasi-one-dimensional flow based on Shapiro's influence coefficients,[23] 2) equilibrium combustion, and 3) frictionless and mass-averaged intake flow, and 4) frozen nozzle flow and reaction kinetics for supersonic combustion and nozzle expansion. The combustion efficiency is assumed to be 0.98, and the vehicle flies a constant dynamic pressure trajectory of 1000 psf. The geometry of the combustor is represented by a dual-mode RJ/SJ configuration, illustrated in the schematic of Fig. 6, where the different station numbers represent the various stages in the SJ combustor.

The station numbers 3 and 4 on Fig. 6 designate burner entry and exit sections. Station 2 is the entry to the isolator, whereas station 3 is the exit of the isolator, start of the combustor, and the axial location of fuel injection. Station 10 represents the end of the nozzle expansion. The flow at station 2 has been compressed by the bow and ramp shock and the reflected shock off the cowl lip.

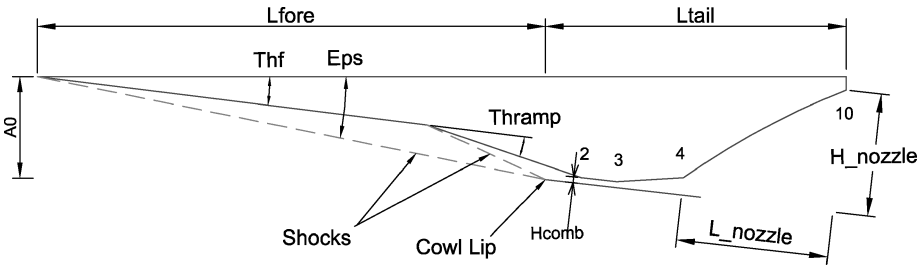

Fig. 6 Key geometric parameters in waverider design.

At flight Mach numbers greater than 5, excessive chemical dissociation can occur as a result of the high static temperatures caused by inefficient inlet compression. This can reduce the combustion heat release and the net thrust.[21] For flight Mach numbers less than 5, the flow must be subsonic, and the combustor should operate under ramjet mode; for Mach numbers greater than 5, supersonic combustion occurs, and SJ operation begins.

During subsonic combustor flow, two physical throats are required to first decelerate the flow from supersonic to subsonic and then to accelerate the flow back to supersonic for the expansion nozzle. For SJ operation, no throat is necessary, as the flow remains supersonic throughout. The dual-mode RJ/SJ engine satisfies these modes by using a constant-area section known as an isolator, which effectively operates like a diffuser. Therefore no area constriction is required within the combustor geometry. The height of the isolator is represented by H_i.

The isolator is positioned between stations 2 and 3 and prevents undesirable inlet-combustor interactions by containing the precombustion shock structure. A significant problem in practical SJ operation is maintaining the pressure at station P_2 above the combustor backpressure P_3; otherwise, flow separation can occur as a result of thermal occlusion. The length of isolator should therefore be long enough so that the shock train does not migrate upstream of the isolator and cause inlet unstart. To choke the flow and fix P_3 requires the correct combination of A_x, fuel-air mixing, and combustion T_{tx}.

The isolator can also function during supersonic combustion. If during heat addition and area increase, thermal occlusion occurs, then the wall boundary layer can separate. The isolator can contain the oblique shock train and prevents the adverse pressure gradient unstarting the inlet. This is assuming that the isolator exit has a supersonic confined core flow surrounded by a region of separated flow.[24,25] The core flow reattaches at the axial location of maximum pressure.

The variation of Mach number through the combustor is given by Eq. (3) with a linear divergent change in a user-defined area A_x and T_{tx}. This is based on calorically perfect gases with prescribed specific heat ratios, frictionless flow without mass addition, and constant pressure heat addition.

$$\frac{\mathrm{d}M_x}{\mathrm{d}x} = M_x \left\{ \frac{1 + [(\gamma_b - 1)/2]M_x^2}{1 - M_x^2} \right\} \times \left[-\left(\frac{1}{A_x} \frac{\mathrm{d}A_x}{\mathrm{d}x} \right) + \frac{1 + \gamma_b M_x^2}{2} \left(\frac{1}{T_{\text{tx}}} \frac{\mathrm{d}T_{\text{tx}}}{\mathrm{d}x} \right) \right] \tag{3}$$

This ordinary differential equation is integrated step by step using a fourth-order Runge–Kutta technique. Pressure, temperature, and velocity as a function of axial position can be calculated using rational functions given by Shapiro.[23] Thermal choking can thus occur at an axial location where $M = 1$.

Several assumptions have been made in the combustor analysis.[26] The combustor is a rectangular modular engine that is highly integrated into the waverider lower undersuface. Combustion occurs at constant pressure. The concept is likely to use swept compression surfaces and fuel injector struts to provide inlet starting at low speed and good internal performance throughout the SJ operating speed range. Instream fuel injection is used to minimize combustor length and heat flux to the internal surfaces. Uniform two-dimensional flow exhausting from a single combustor exit with frozen chemistry was assumed to represent the engine package. The heat released during combustion is based on complete combustion occurring from initial conditions.

Hydrogen is the preferred fuel at hypersonic Mach numbers as a result of its high-performance yield, low-molecular-weight-producing high specific impulse and rapid ignition, reaction, and combustion. It is also kinder to the environment as it produces low environmental pollutants because the major biproduct of combustion is water vapor. If the combustor length is too long, the takeoff weight increases, and specific impulse decreases. The length cannot be shorter than required for establishing complete mixing of fuel and air to produce the desired stoichiometric conditions. Because the flows within these combustors are supersonic, the mixing and residence time available for reaction are reduced compared to subsonic combustors. Its length is estimated using an analytical expression for the reaction time as a function of combustor entrance conditions.[15]

The cryogenically stored hydrogen provides regenerative cooling, and a good heat-sink capacity for the leading edges of hot structure and the combustor walls. Hydrogen, however, has a lower density than hydrocarbon fuels and requires a larger vehicle volume for storage.

The key to success in the design of a SJ is the proper mixing of hydrogen fuel and high-speed air while combusting the mixture before it exits the vehicle. Enough thrust must be produced to overcome the drag of the vehicle. The walls of the combustor need to be adequately cooled, and this is possible by reducing the pressure and wetted surface through the use of separated bubbles.

The mixing length is a boundary condition for the separation and reattachment process. Oblique shocks present in the combustor can cause separation, and this can be predicted by using boundary-layer separation criteria, $M_d/M_u < 0.762$, to approximate for turbulent boundary layers.[22,24]

Reliable combustor operation requires continuous ignition to effect flame holding. As discussed by Ortwerth,[27] flame holding is provided by a recirculation zone from the separation around a fuel jet.

This quasi-one-dimensional model has previously[6] been validated with experimental data from tests of Billig and Grenleski,[28] and the model used in this investigation with regards to the preceding assumptions produced an average error of 9.3%.

The Mach-number variation and the change in pressure and temperature through the SJ combustor are shown in Fig. 7 for Mach 9 flight. A_x/A_2 increases linearly by factor of two relative to the area of the isolator exit at station 3. The constant pressure occurs as the maximum pressure transmits upstream through the separated region near the walls where it impinges on the confined core flow. The temperature increases from station 3 onwards as a result of heat addition. Heat addition does not always initiate with fuel injection because of mixing delays.

Other methodologies specific to SJ analysis and design are the performance prediction method by Ikawa[29] that uses a first-order

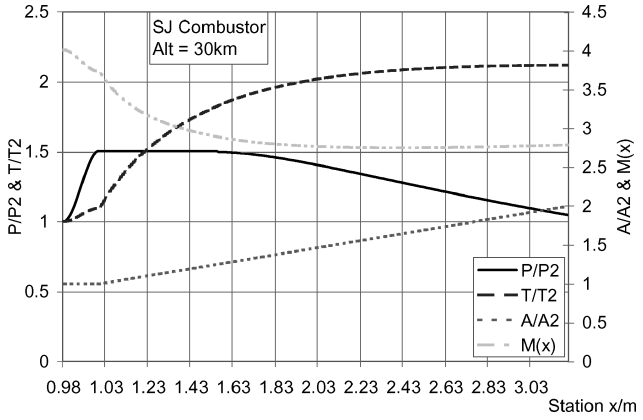

Fig. 7 Various thermodynamic flow properties through SJ combustor.

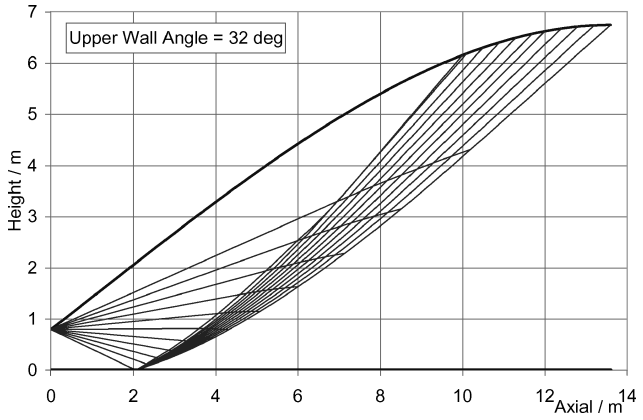

Fig. 8 Nozzle characteristic mesh.

approximation for the supersonic combustor analysis, which is similar to the approach of afterburning in a RJ. A multiplying factor has been introduced by Ikawa that eliminates the need for numerical integration solving for divergent channel flow. A simplified model using fundamental physics is developed by Schindel[30] for predicting performance of missile configurations. Combustion is assumed to be a continuous process with constant-area heat addition.

Nozzle

The length and height of the nozzle, as shown on Fig. 6, are determined by subtracting the dimensions of the forebody and combustor length from the total vehicle length, set at 60 m for the purpose of this study. The combustor exit flow is treated as steady and irrotational and considered to be uniform across the span of the engine, maintained by holding a constant spanwise upper wall angle. The contour of the nozzle is defined by a third-order polynomial and by setting the initial and final wall angles.

Using the preceding assumptions, the characteristic equations are considered hyperbolic, and the two-dimensional method of characteristics can be used to compute the nozzle flowfield.[31] The algebraic compatibility equation, which is indeterminate along a characteristic line, is defined by Eq. (4):

$$C_{\pm} = \delta \mp v(M) \tag{4}$$

Two expansion fans are used to define the nozzle, one emanating from the upper wall and the other is the cowl chamfer with a set angle of 6 deg (Ref. 26). The upper-wall angle is allowed to vary iteratively until the boundaries of the nozzle are achieved. The location of the cowl extension into the nozzle is set by the first characteristic emanating from the upper wall. Greater thrust is produced if the cowl is allowed to extend further than this point, but this would also increase drag. A characteristic mesh for Mach 9 flight with $M_4 = 2.8$ is shown in Fig. 8.

The exhaust flow is often underexpanded because of the losses incurred during the inlet compression and eventual combustion. To achieve high thrust, correct trim, and low system weight, the shape of the nozzle/aftbody needs to be optimized for the available height and length. This is possible within HICAD by varying the nozzle upper-wall angle such that the pressure and Mach exiting the nozzle geometry produces a high thrust value.

Idealized Turboramjet Analysis

For the low-speed regime, a TBCC engine was selected for the propulsion device to accelerate the vehicle from takeoff to SJ transition. Existing research studies[6,32,33] examine the potential of a TRJ to meet this requirement. In addition the Japanese ATREX engine[8] is a fan-boosted ramjet designed to produce thrust at sea-level static to Mach 6 flight. Idealized analysis of a TRJ was carried out using the method formulated by Heiser and Pratt.[24] It assumes no friction and heat transfer to the walls, and the flow is treated as steady and compressible.

An alternative propulsion system that operates across the full Mach-number range includes the RBCC engine. This engine provides thrust for low speed and high speed and transitions to air-breathing mode when the combustor ceases to provide sufficient thrust. This device has not been considered for the purpose of this study.

The TRJ generates static thrust at takeoff and subsonic speeds by mechanically compressing the air for stable combustion of fuel. The prominent components making up an axisymmetric TRJ are illustrated in the schematic of Fig. 9.

The core of the engine contains a turbojet, which produces high temperature and pressure gases. The turbojet flow is referred to as the primary stream as the turbine operates independent of the flight conditions. The turbines operate to provide power to the fan, which takes air from the inlet and produces a pressure ratio. The compression process to the fan inlet and turbine is treated as isentropic, and there is no loss in efficiency between the two.

Aft of the primary stream, the outer airflow and primary stream are mixed, thereby increasing the total temperature of the flow. The turbine exit is assumed to have no unreacted fuel, and complete mixing occurs before additional fuel is injected as shown on the schematic. Mixers disperse this additional unreacted fuel throughout the air before it is combusted in the burner that includes flameholders. There is no pressure loss as a result of combustion. The injection of fuel in this analysis is considered analogous to afterburning in turbojets. The total temperature of the flow increases and expands isentropically to the freestream static pressure.

The influence of the fan on the airflow is defined by $\pi_F = p_{t3}/p_{t2}$. The method requires inputs for p_{tp}/p_0 and T_{tp}/T_0 as a function of the primary flow. The choices of these variables are iterated until suitable values for thrust matching are achieved for the Mach 5 SJ transition speed. The mass flow of the primary stream and injected fuel are included in the analysis.

Next α is computed, which calculates the ratio of the airflow from the fan to the primary flow and is given by the following expression:

$$\alpha = \frac{T_{\text{tp}}}{T_0} \cdot \frac{T_0}{T_{t0}} \left[\frac{1 - (\pi_F \cdot p_{t0}/p_0 \cdot p_0/p_{\text{tp}})^{(\gamma-1)/\gamma}}{\pi_F^{(\gamma-1)/\gamma} - 1} \right] \tag{5}$$

When the freestream Mach number becomes large, α eventually reaches zero as shown in Fig. 10. This occurs when the quantity

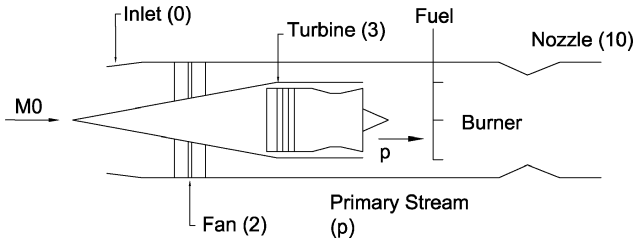

Fig. 9 Schematic of TRJ propulsion system.

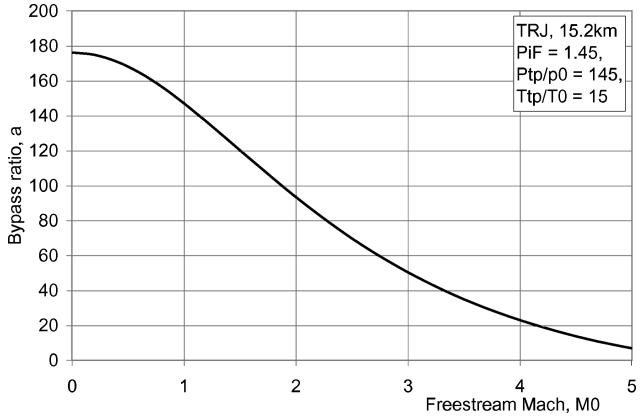

Fig. 10 Limit of the TRJ airbreathing segment indicated by the bypass ratio tending to zero.

$\pi_F(p_{t0}/p_0) = p_{\text{tp}}/p_0$ in the numerator of Eq. (5). At this point the device is considered to behave like a rocket as the flow is entirely caused by the primary flow, and so airbreathing performance measures such as F/m_0 no longer have physical meaning. For the purpose of this study, this is considered to be the limit of the TRJ model.

To achieve Mach 5, α needs to remain nonzero within the Mach range considered. If the military specification for the total pressure recovery MIL-E-5008B p_{t2}/p_{t0} is applied to the fan airflow for supersonic M_0, then this limit point can be delayed.

$$p_{t2}/p_{t0} = 1 - 0.075(M_0 - 1)^{1.35} \tag{6}$$

Furthermore, the diminishing P_0 that accompanies flying at increasing altitudes increases the value of p_{tp}/p_0 and T_{tp}/T_0, which has a favorable effect in achieving higher Mach numbers under TRJ power.

To achieve thrust matching of the TRJ and SJ engine, the thrust of the two engines need to be adjusted so that a continuous transition occurs between them. This is achieved by iterating on the preceding parameters within specified constraints, which include a peak value of $I_{\text{sp}} = 4000$ s from available literature. This in turn provides data for F/m_0 as a function of h. The TRJ F/m_0 is found at the desired SJ transition point at Mach 5 and $h = 30$ km, and a value for $\dot{m}_0$ is determined in order to achieve the desired thrust in Newtons for the SJ. This is also dependent on the number of engines, with a limit currently placed on four engine units. The design $\dot{m}_0$ is restricted such that the size of the inlet $A_{0\text{ref}}$ does not exceed realistic limits and those imposed by the design.

After achieving the desired performance matching of the low-speed and high-speed engine, a suitable external compression inlet needs to be designed for the TRJs. The inlet should 1) provide the necessary airflow for the TRJ from low-subsonic to high-supersonic flight conditions at all altitudes considered, 2) deliver high η_R, 3) ensure off-design conditions are fully met, and 4) minimize losses. In particular, the defined inlet should provide the necessary $\dot{m}_0$ to achieve the desired thrust for SJ transition. An off-design cycle analysis code OFFX[34] is used to determine the corrected engine airflow vs both M_0 and h. OFFX defines the requirement of the inlet in terms of its total pressure ratio based on Eq. (6) and $\dot{m}_0$.

A four-ramp variable geometry inlet with four different ramp angles, one of which is the forebody ramp angle shown in Fig. 11, was selected to generate good values of η_R over the desired flight speed range while maintaining the shock-on-lip and sonic throat conditions.

The inlet design begins with an analysis of the required inlet airflow.[34] As part of the multidisciplinary nature of the methodology, OFFX can be operated from within HICAD. By selecting a TRJ sizing point of Mach 2.5 at $h = 15.2$ km with $\dot{m}_0 = 136.1$ kg/s, the corresponding values of A_0 are calculated using OFFX at any other specified M_0 and h. Other variables used for optimization include

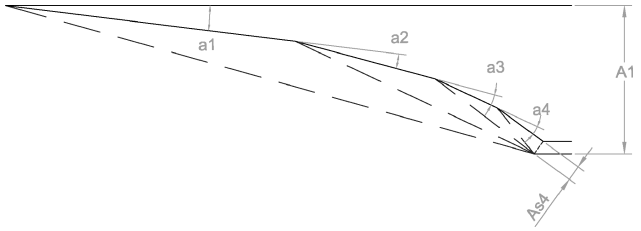

Fig. 11 TurboRamjet inlet Mach 5, $h = 30$ km.

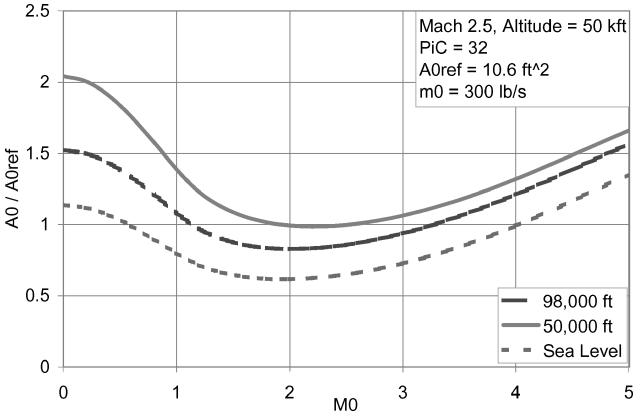

Fig. 12 Required inlet airflow at various altitudes.

the fan compressor ratio. The design case determines the reference area $A_{0\text{ref}}$, and using $\dot{m}_0$ vs M_0 data from OFFX at different h, an airflow requirement plot $A_0/A_{0\text{ref}}$ is produced like that shown in Fig. 12, which has a minimum around Mach 2. The flight conditions are shown in the insert of the figure.

This figure presents information to select the flight condition at which the mass flow requirement at a particular Mach number is the greatest. The area ratio A_{0i}/A_{s4} is then determined by the following equation given that $\eta_R = P_{t5}/P_{t0}$:

$$\frac{A_{0_i}}{A_{s4}} = \eta_R \frac{A/A^*|_{M_0}}{A/A^*|_{M_5}} \tag{7}$$

The required throat area A_{s4} can then be determined from $A_{s4} = A_{0i\text{req}}/(A_{0i}/A_{s4})$. Finally $A1$ is calculated from geometry for a given value of A_{s4}. The value of $A1$ is a function of the geometric ramp angle configuration, and its final value is found when the highest value of η_R is achieved and M_4 is greater than unity thus providing subsonic flow for the combustor.

Having determined $A1$, the ramp angles for the range of Mach numbers that lead to the best pressure recovery can be found. Given the large number of possible ramp angles, the selected configuration is based on equal strength shocks translating as an equivalent total pressure ratio across each shock. The pressure recovery at the design point should, at least, exceed Eq. (6). Figure 13 shows the pressure recovery over the Mach range for low-speed operation at the transition altitude of 50,000 ft. The inlet has a greater pressure recovery than p_{t2}/p_{t0} given by Eq. (6) appropriate for subsonic combustion RJs.

The model assumes intake operation with five shocks to define the total pressure recovery factor. Because additive spillage drag forces and effects of ingested vehicle forebody boundary layer have not been accounted for, the model might appear a little optimistic.

Lift- and-Drag Estimation Methods

The cruise vehicle will be most efficient if its L/D is maximized. To calculate L/D, a force accounting procedure is adopted. The nonlinear Nelder and Mead method was adopted for this approach.[35] A control volume for the combustor is used to calculate lift, drag, and thrust on the vehicle surface. Not all surfaces are required to calculate L/D. For example, lift produced on the forebody and

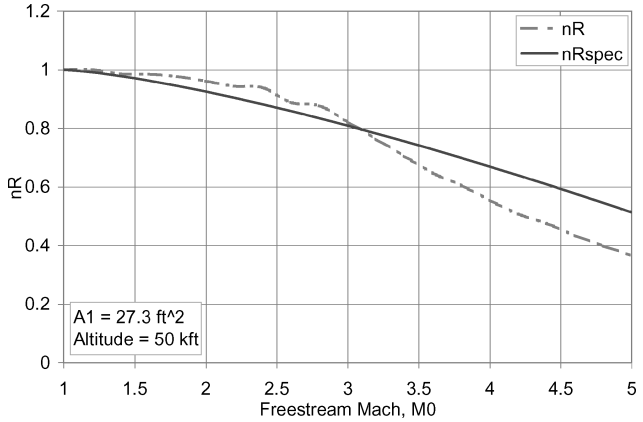

Fig. 13 Intake loss associated with a four-ramp inlet system.

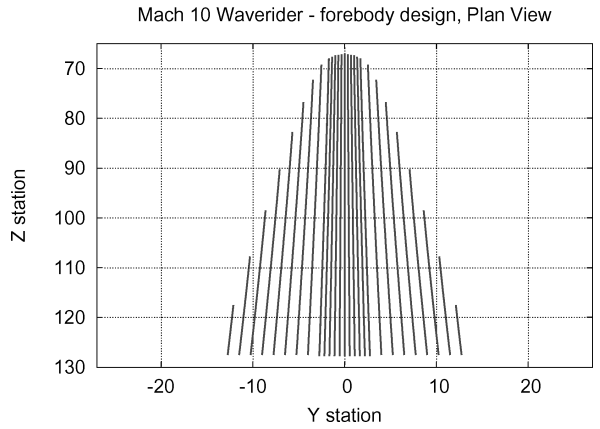

Fig. 14 Plan view of *L/D* maximized Mach 10 waverider.

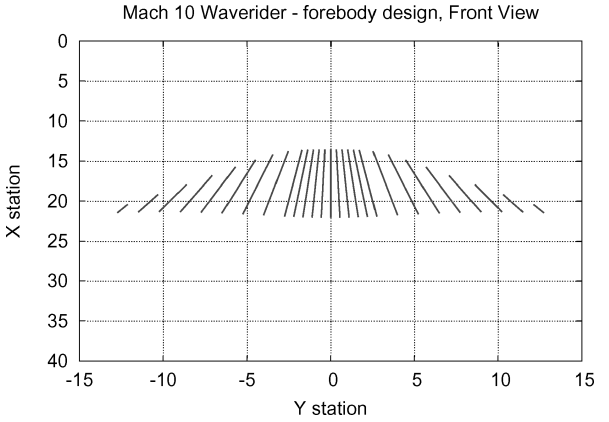

Fig. 15 Front view of *L/D* maximized Mach 10 waverider.

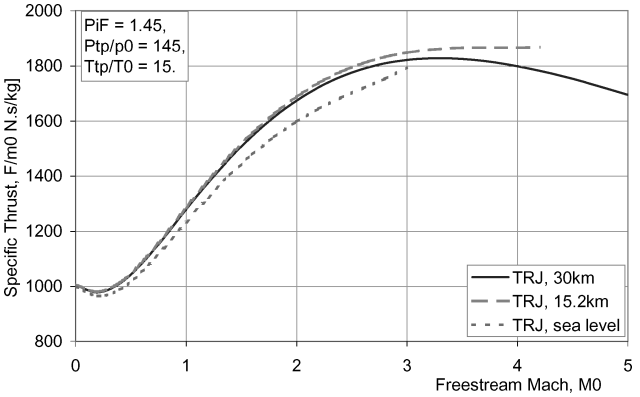

Fig. 16 Specific thrust at different altitudes.

the inlet ramp in the region constrained by W_{eng} is negated by the negative lift acting on the inside surface of the cowl and engine. Therefore, in the engine span region the surfaces that contribute to lift are the cowl exit area and the nozzle upper wall. The wing curve region from nose to tail will also contribute to lift.

All surfaces are used for the drag estimation including the top surface, entire span of forebody, and cowl. Thrust is produced from the cowl, nozzle, and engine, and for the plots illustrated in the following section the thrust is quoted as a single value.

With the assumption that the flow over the waverider is turbulent, the viscous contribution to the force is determined by Eckerts reference temperature method.[36] The forces on each element on the surface of the vehicle are calculated by averaging the pressure and shear stress acting on the vertices of that element. All viscous drag forces are included in the analysis apart from the base drag, which is ignored with the condition that the base is at freestream pressure.

Presented in Fig. 14 is the plan view of a Mach 10 pure waverider shape, and the front view is shown in Fig. 15. This configuration geometry produces an $L/D = 7.8$. The span of the engine was 5 m in the inlet plane. This value does not include the integration of engine and nozzle, which is currently under investigation.

Variables optimized for the preceding figures were the inlet curve and wing curve shape to produce maximum L/D configurations. These are constrained by an outer limit of the conical shock and inner limit of its corresponding cone surface. A change in the ellipticity of the inlet curve produced a more pointed nose as Mach number increased for L/D maximized waveriders.

Thrust-Matching Results

The TRJ and SJ are integrated in an over/under configuration, which appears to be the most suitable arrangement for a TBCC and SJ in terms of flow-path integration.[37] The pressure recovery graph shown in Fig. 13 has a total flow turning angle of 36 deg at Mach 5 and $h = 30$ km. η_R can be improved by allowing a greater turning angle at this case, but this will increase drag. The inlet for the TRJ is integrated with the SJ with flow diverters such as movable flaps to direct the air to the TRJ for Mach numbers between $0 < M_0 \leq 5$ and to the SJ for $5 < M_0 < 10$ with a transition phase around Mach 5, where a parallel operation of the TRJ and SJ is anticipated. Rectangular inlet designs are generally easier for airframe integration. The thrust data represent uninstalled thrust.

The specific thrust graph (Fig. 16) provides the data to determine the mass flow ratio required to achieve the desired thrust at the SJ transition speed of Mach 5 at 30 km. The plot is obtained using stream thrust analysis, which takes the fuel/air ratio as one of its parameters. It relies on momentum relationships and a control volume that represents the on-design freestream capture area to nozzle-exit area. It is assumed that velocity vector is aligned with the local axial direction with the through-flow area perpendicular to that direction. The thrust produced by the SJ during constant altitude acceleration is shown in Fig. 17 along with the thrust curves for the TRJ at different altitudes. Four TRJ units are used, each with a design $\dot{m}_0 = 136$ kg/s that translates to a reference area of $A_{0_{\text{ref}}} = 0.98$ m^2. The thrust is calculated as a product of the specific impulse and $\dot{m}_0$, which is obtained from the low-speed inlet analysis.

The TRJ displays high values for I_{sp} at midrange supersonic Mach numbers as shown in Fig. 18. The I_{sp} graph is matched with the SJ through iteration of the primary flow variable as described in a preceding section. I_{sp} is a function of F/m_0 given by the following equation:

$$I_{\text{sp}} = 1/g_0(f + 1/\alpha) \cdot F/\dot{m}_0 \tag{8}$$

where $g_0 = 32.174$ ft/s^2. Any matching of I_{sp} has to maintain the thrust matching for the SJ, and HICAD performs this by undergoing an iteration procedure.

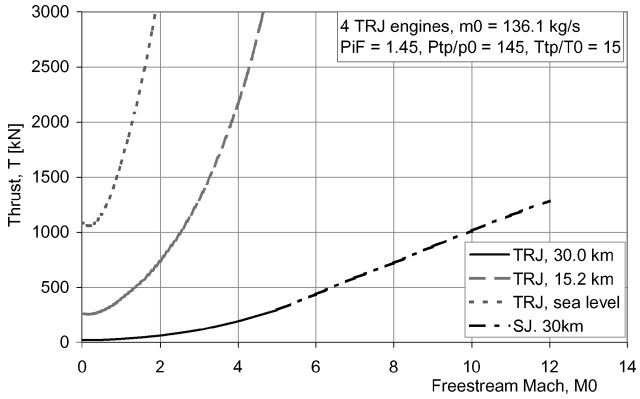

Fig. 17 Thrust matching of low-speed and high-speed engine.

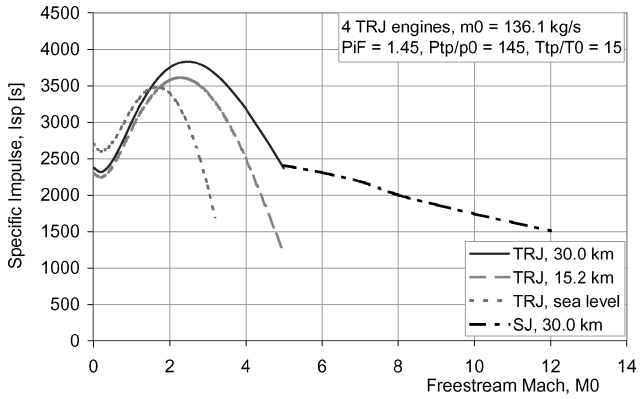

Fig. 18 Specific impulse variation at different flight altitudes.

The objective of the low-speed system is to provide adequate thrust for takeoff and transonic/supersonic acceleration to the high-speed propulsion system transition Mach number. The low-speed system will cease operation above transition so that mechanisms need to be employed to stop the airflow through the low-speed inlet system and divert it to the SJ during hypersonic flight. The nozzle is also highly integrated with the SJ nozzle and operates only during TRJ operation.

Conclusions

The smooth thrust transition between a TRJ and a SJ was demonstrated through idealized cycle analysis. Four TRJ units were sized along with their inlets and integrated with the SJ. A conically derived waverider was selected as the baseline configuration for this study because of its readiness in integration with a SJ and the favorable L/D ratio it generates at the on-design condition. A Mach 10 L/D maximized waverider generated a value of $L/D = 7.8$.

This waverider-derived configuration is providing convenient integration with the TRJ/SJ propulsion combination, needed for both low- and high-speed operation, respectively. The presented methodology provides a step-by-step procedure for achieving a valid propulsion/airframe integration at the initial design stage and helps to establish the desired thrust matching at transition speed.

Hypersonic vehicles are highly integrated systems requiring unconventional design approaches and multivariable analysis. The work shown forms part of an initial design methodology for practical hypersonic cruise aircraft concepts with low-speed, horizontal takeoff and landing capabilities.

HICAD's development will continue in order to provide low-speed aerodynamic data, initial sizing, weights, systems packaging, stability, and performance. The methodology will be optimized in order to converge on the most efficient solution for hypersonic cruise flight. It will include complete force estimation and integration of individual components and will aim to maximize the overall vehicle L/D including the nozzle, top surface, and the cowl.

The current study focuses on the on-design cruise case only for the hypersonic regime, and further investigation will be carried out to look at variable inlet geometry and off-design performance. The vehicle currently flies on a constant dynamic pressure trajectory and will be improved when the low-speed aerodynamic performance is fully addressed.

The methodology is limited to the conically derived waverider, which has a smaller vehicle volume compared to equivalent osculating-cone concepts and could be extended to test the run time for optimized configurations. Other variables will be included to extend the optimization investigation such as the engine size and the axial location of the inlet plane for example.

References

[1]Bertin, J. J., and Cummings, R. M., "Fifty Years of Hypersonics: Where We've Been, Where We're Going," *Progress in Aerospace Sciences*, Vol. 39, Nos. 6–7, 2003, pp. 511–536.

[2]Dornheim, M. A., "A Breath of Fast Air," *Aviation Week and Space Technology*, Vol. 160, No. 14, April 2004, pp. 28, 29.

[3]Nonweiler, T., "Aerodynamic Problems of Manned Space Vehicles," *Journal of the Royal Aerounautical Society*, Vol. 63, No. 585, Sept. 1959, pp. 521–528.

[4]Bowcutt, K., Anderson, J., and Capriotti, D., "Viscous Optimized Hypersonic Waveriders," AIAA Paper 87-0272, Jan. 1987.

[5]Pegg, R. J., Hunt, J. L., and Petley, D. H., "Design of a Hypersonic Waverider-Derived Airplane," AIAA Paper 93-0401, Jan. 1993.

[6]O'Neill, M. K. L., "Optimized Scramjet Engine Integration on a Waverider Airframe," Master's Thesis, Dept. of Aerospace Engineering, Univ. of Maryland, College Park, Aug. 1992.

[7]Takashima, N., and Lewis, M. J., "Optimization of Waverider-Based Hypersonic Cruise Vehicles with Off-Design Considerations," *Journal of Aircraft*, Vol. 36, No. 1, 1999, pp. 235–245.

[8]Tanatsugu, N., "Development Study on Air TurboRamjet," *Developments in High-Speed-Vehicle Propulsion Systems*, edited by S. Murthy and E. Curran, Progress in Astronautics and Aeronautics, Vol. 165, AIAA, Reston, VA, 1996, pp. 259–332.

[9]Moses, P. L., Bouchard, K. A., Vause, R. F., and Pinckney, S. Z., "An Air-breathing Launch Vehicle Design with Turbine-Based Low-Speed Propulsion and Dual Mode Scramjet High-Speed Propulsion," AIAA Paper 99-4948, Nov. 1999.

[10]Bowcutt, K. G., "A Perspective on the Future of Aerospace Vehicle Design," AIAA Paper 2003-6957, Dec. 2003.

[11]Harloff, G., and Berkowitz, B., "HASA—Hypersonic Aerospace Sizing Analysis for the Preliminary Design of Aerospace Vehicles," NASA CR 182226, Nov. 1988.

[12]Chaput, A. J., "Preliminary Sizing Methodology for Hypersonic Vehicles," *Journal of Aircraft*, Vol. 29, No. 2, 1992, pp. 172–179.

[13]Carreiro, L., "PDWAP—A Preliminary Design and Weights Analysis Program for Aerospace Vehicles," Tech. Rept. AD-A222 614, Wright–Patterson AFB, Ohio, Jan. 1990.

[14]Molvik, G., Bowles, J., and Huynh, L., "Analysis of a Hypersonic Research Vehicle with a Hydrocarbon Scramjet Engine," AIAA Paper 93-0509, Jan. 1993.

[15]O'Brien, T. F., and Lewis, M. J., "Rocket-Based Combined-Cycle Engine Integration on an Osculating Cone Waverider Vehicle," *Journal of Aircraft*, Vol. 38, No. 6, 2001, pp. 1117–1123.

[16]Horton, I., *Beginning Visual C++ 6*, Wiley, New York, 1998, Chaps. 13–18.

[17]Espinosa, A. M., "Hypersonic Airbreathing Propulsion: Mach 10 Cruiser Conceptual Design/Integration," AIAA Paper 93-4735, Aug. 1993.

[18]Cockrell, C. R., Auslender, A. H., and McClinton, C. R., "Technology Roadmap for Dual-Mode Scramjet Propulsion to Support Space-Access Vision Vehicle Development," AIAA Paper 2002-5188, Sept.–Oct. 2002.

[19]Sobieczky, H., Dougherty, F., and Jones, K., "Hypersonic Waverider Design from Given Shock Waves," *Proceedings of the 1st International Hypersonic Waverider Symposium*, Univ. of Maryland, College Park, MD, 1990.

[20]Takashima, N., and Lewis, M., "Waverider Configurations Based on Non-Axisymmetric Flow Fields for Engine-Airframe Integration," AIAA Paper 94-0380, Jan. 1994.

[21]Anderson, G., McClinton, C., and Weidner, J., "Scramjet Performance," *Scramjet Propulsion*, edited by S. Murthy and E. Curran, Progress in Astronautics and Aeronautics, Vol. 189, AIAA, Reston, VA, 2000, pp. 597–695.

[22]Billig, F. S., "Research on Supersonic Combustion," *Journal of Propulsion and Power*, Vol. 9, No. 4, 1993, pp. 499–514.

[23]Shapiro, A. H., *The Dynamics and Thermodynamics of Compressible Fluid Flow*, Vol. I, Ronald, New York, 1953, pp. 219–231.

[24]Heiser, W. H., and Pratt, D. T., *Hypersonic Airbreathing Propulsion*, AIAA, Washington, DC, 1994, pp. 277–385.

[25]Waltrup, P., and Billig, F., "Prediction of Precompression Wall Pressure Distributions in Scramjet Engines," *Journal of Spacecraft and Rockets*, Vol. 10, No. 9, 1973, pp. 620–622.

[26]Small, W. J., Weidner, J. P., and Johnston, P., "Scramjet Nozzle Design and Analysis as Applied to a Highly Integrated Hypersonic Research Airplane," NASA TN D-8334, Nov. 1976.

[27]Ortwerth, P., "Scramjet Flowpath integration," *Scramjet Propulsion*, edited by E. Curran and S. Murthy, Progress in Astronautics and Aeronautics, Vol. 189, AIAA, Reston, VA, 2000, pp. 1105–1290.

[28]Billig, F., and Grenleski, S., "Heat Transfer in Supersonic Combustion Processes," *Heat Transfer 1970*, Vol. III, Elsevier, Amsterdam, Aug. 1970, pp. 1–11.

[29]Ikawa, H., "Rapid Methodology for Design and Performance Prediction of Integrated Supersonic Combustion Ramjet Engine," *Journal of Propulsion and Power*, Vol. 7, No. 3, 1991, pp. 437–444.

[30]Schindel, L. H., "Design Model of High-Performance Ramjet or Scramjet-Powered Vehicles," *Journal of Spacecraft and Rockets*, Vol. 27, No. 6, 1990, pp. 613–617.

[31]John, D., and Anderson, J., *Modern Compressible Flow: with Historical Perspective*, international ed., McGraw–Hill, Singapore, 1990, pp. 311–331.

[32]Hunt, J., Pegg, R., and Petley, D., "Airbreathing Hypersonic Vision-Operational-Vehicles Design Matrix," Society of Automotive Engineers, 1999-01-5515, Oct. 1999.

[33]Hewitt, F., and Johnson, M., "Propulsion System Performance and Integration for High Mach Air Breathing Flight," *High-Speed Flight Propulsion Systems*, edited by S. Murthy and E. Curran, Progress in Astronautics and Aeronautics, Vol. 137, AIAA, Washington, DC, 1991, pp. 101–142.

[34]Mattingly, J. D., Heiser, W. H., and Daley, D. H., *Aircraft Engine Design*, AIAA, New York, 1987, pp. 353–395.

[35]Nelder, J., and Mead, R., "A Simplex Method for Function Minimization," *Computer Journal*, Vol. 7, Jan. 1965, pp. 308–313.

[36]Eckert, E., "Engineering Relations for Heat Transfer and Friction in High-Velocity Laminar and Turbulent Boundary-Layer Flow over Surfaces with Constant Pressure and Temperature," *Transactions of the ASME*, Vol. 78, Aug. 1956, pp. 1273–1283.

[37]Javaid, K. H., and Serghides, V. C., "Thrust-Matching Requirements for the Conceptual Design of Hypersonic Waverider Vehicles," AIAA Paper 2003-6953, Dec. 2003.